Biomimetic *S*-adenosylmethionine regeneration for nucleophilic and radical alkylation reactions and aminopropyltransfer

Lukas Gericke,[§,1] Dipali Mhaindarkar,[§,1] Lukas Karst,[§,1] Sören Jahn,[1] Marco Kuge,[1] Michael K. F. Mohr,[1] Jana Gagsteiger,[2] Nicolas V. Cornelissen,[3] Xiaojin Wen,[4] Silja Mordhorst,[1,5] Henning J. Jessen,[6] Andrea Rentmeister,[3] Florian P. Seebeck,[4] Gunhild Layer,[2] Christoph Loenarz,[1] Jennifer N. Andexer[1*]

[1] Institute of Pharmaceutical Sciences, Pharmaceutical and Medicinal Chemistry, University of Freiburg, Albertstr. 25, 79104 Freiburg, Germany

[2] Institute of Pharmaceutical Sciences, Pharmaceutical Biology, University of Freiburg, Stefan-Meier-Str. 19, 79104 Freiburg, Germany

[3] Department of Chemistry, Institute of Biochemistry, University of Münster, Corrensstr. 36, 48149 Münster, Germany

[4] Department of Chemistry, University of Basel, Mattenstr. 22, 4058 Basel, Switzerland

[5] Present address: Pharmaceutical Institute, Pharmaceutical Biology, University of Tübingen, Auf der Morgenstelle 8, 72076 Tübingen, Germany

[6] Institute of Organic Chemistry, University of Freiburg, Albertstr. 21, 79104 Freiburg, Germany

[§] Equal contributions

* To whom correspondence should be addressed. Tel: +49 761 203 6341; Fax: +49 761 203 6351; Email: jennifer.andexer@pharmazie.uni-freiburg.de.

Abstract

S-Adenosylmethionine (SAM) is an essential and versatile cofactor in nature. SAM-dependent enzymes, such as conventional methyltransferases (MTs), amino(carboxy)propyl transferases, and radical SAM enzymes, are of great interest as biocatalytic tools for chemical synthesis and the pharmaceutical industry. The use of SAM analogues adds to the diversity of reaction types and products. While SAM regeneration protocols for conventional MTs are available, *in vitro* SAM regeneration for polyamine-forming enzymes and radical SAM enzymes has not been solved yet. Here, we report a biomimetic cofactor regeneration cycle for three important types of SAM-dependent enzymes featuring adenine as a central intermediate. SAM is regenerated from its main degradation products, *S*-adenosylhomocysteine, 5′-methylthioadenosine, and 5′-deoxyadenosine. We further show the chemical diversification of the system using SAM analogues such as *S*-adenosylethionine for MT reactions. Interestingly, the enzyme cascades also enable the transfer of an ethyl group with a cobalamin-dependent radical SAM MT. The possibility to regenerate SAM (analogues) for biocatalytic use with a broad range of enzymes will be a starting point for further application of

the diverse chemistry accessible by SAM-based catalysis, as well as provide new options for mechanistic studies.

Introduction

S-adenosylmethionine (SAM, AdoMet) is one of the most abundant and versatile enzyme cofactors. The sulfonium ion is widely known as one of nature's methyl group donors and for its role in the biosynthesis of a wide range of natural products.[1–3] Methylation is essential for epigenetic regulation *via* nucleobase and histone methylation and consequently closely connected to human health and disease.[4,5] Especially in drug synthesis, methylation is a highly effective modification that can increase the potency of a substance up to three orders of magnitude, leading to the term "magic methyl effect".[6,7] SAM-dependent enzymes have the potential to provide an environmentally friendly alternative to commonly used toxic, and potentially unselective alkylating agents.[8]

Conventional SAM-dependent methyltransferases (MTs, E.C. 2.1.1) use SAM as a methyl donor with a nucleophilic substrate in an S_N2 reaction, forming *S*-adenosylhomocysteine (SAH) as a byproduct (Fig. 1a).[1–3] The biosynthesis of many pharmacologically active natural products such as galantamine and caffeine involves MTs (Fig. 1b). In addition, other SAM-dependent enzymes perform versatile reactions while using different substructures of the cofactor.[2,3,9] Aminocarboxypropyl transferases (ACPT, e. g. E.C. 2.5.1.38) transfer the aminocarboxypropyl moiety of SAM to various substrates.[10–12] After decarboxylation of SAM, the aminopropyl side chain provides building blocks for the biosynthesis of polyamines by aminopropyl transferases (APT, e. g. E.C. 2.5.1.16);[13] in both cases, 5′-methylthioadenosine (MTA) is formed as the SAM-derived byproduct (Fig. 1a). Simple linear polyamines such as spermidine and spermine occur in all forms of life; they are important for diverse cellular processes, including apoptosis, cell differentiation, gene expression, homeostasis, and signalling.[13,14] Polyamines are also used as building blocks for polyamine alkaloids with multiple biological functions.[15] This group of natural products contains acylated and alkylated polyamines, as well as compounds containing other building blocks including terpenes and nucleobases. Examples are the cytotoxic compounds motuporanine G-I and the spider toxin PA3334G (Fig. 1c).[15,16]

The discovery of the radical SAM superfamily (PF04055) dramatically increased the scope of SAM-dependent reactions and consequently potential applications. The members of this superfamily use a SAM-derived 5´-deoxyadenosyl radical (DOA•) to initiate radical chemistry for a broad range of synthetically challenging reactions(Fig. 1a).[17] These include methylations at unactivated carbons, other C-C bond formations as well as rearrangements, e. g. ring contractions.[18–21] Radical SAM enzymes are present in the biosynthetic gene clusters of countless natural products, including biotin and the antibiotics gentamicin and phosalacine

(Fig. 1d).[18,22] Alternatively to abstracting a hydrogen atom from the substrate [resulting in 5′-deoxyadenosine (DOA) as a byproduct], the DOA• radical can be added to an alkene resulting in an adenosylation.[23] Regarding methylation reactions, particularly class B radical SAM MTs have gained interest due to their ability to catalyse challenging methylations on sp^3-hybridised C or P atoms.[24–29] In addition to the SAM molecule used to generate the DOA• radical, class B radical SAM MTs utilise an additional SAM to methylate cobalamin, which serves as a methyl shuttle.[30]

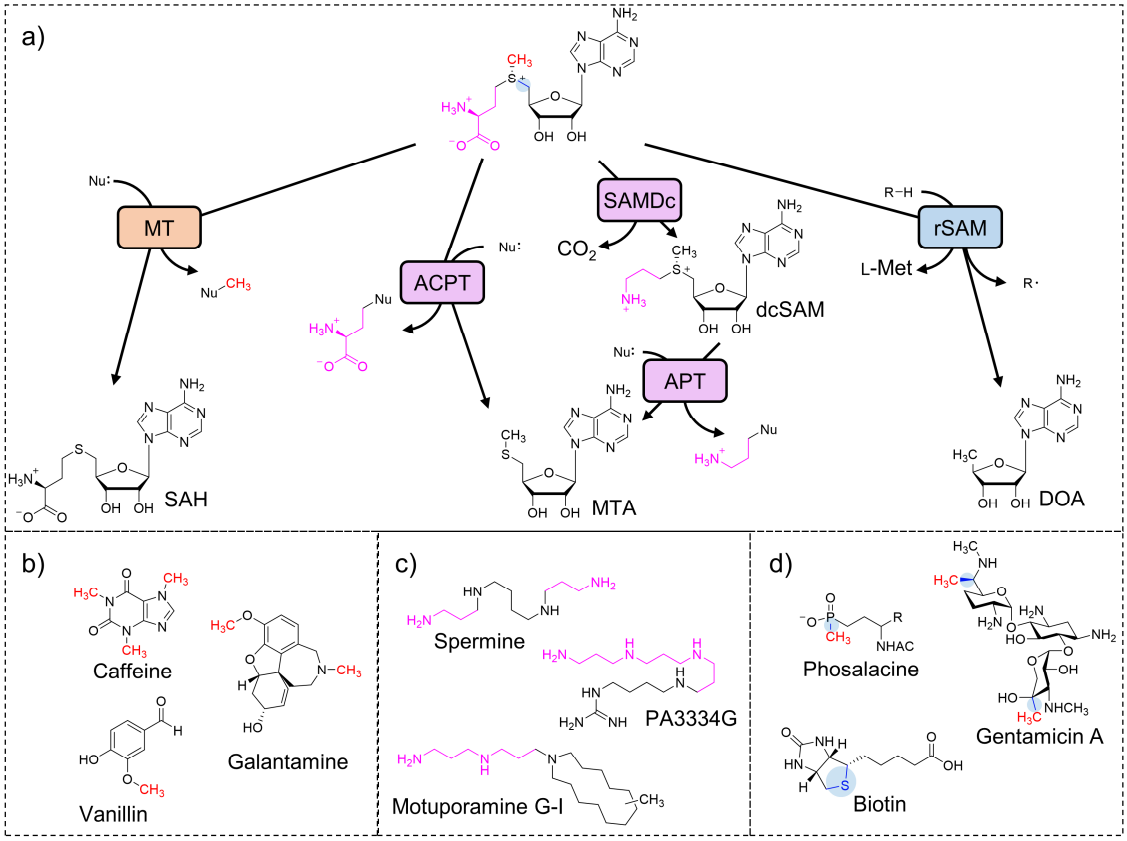

Fig. 1 SAM is a highly versatile cofactor involved in a wide range of reactions. **a)** SAM-dependent enzymes can be divided into three large groups based on the structural moieties transferred: methyl transferases (MT, red), enzymes transferring the aminocarboxypropyl moiety (ACPT) or the aminopropyl moiety (APT) after decarboxylation by SAM decarboxylase (SAMDc) (pink), and radical SAM enzymes (rSAM, blue). The substrate radical is displayed as a common intermediate for the diverse reactions catalysed by radical SAM enzymes. **b)** Examples for methylated drugs and food additives. **c)** Examples for polyamines. **d)** Examples for radical SAM enzyme products.

The diversity of SAM-dependent reactions renders them of great interest for application in organic synthesis and biotechnological processes.[8,23,31,32] However, in addition to the high cost and low stability of the SAM cofactor,[33] in many cases SAM-derived byproducts have an inhibitory effect on the corresponding enzymes.[18,34,35] This encouraged the development of multi-enzyme systems for SAM supply or regeneration. SAM supply usually starts from L-methionine (L-Met) and 5´-adenosine triphosphate (ATP) using methionine adenosyltransferase (MAT, E.C. 2.5.1.6), nature's SAM-synthesising enzyme.[36,37]

Alternatively, chlorinases (E.C. 2.5.1.94) are employed to synthesise SAM from L-Met and 5′-chloro-5′-deoxyadenosine (CldA) in their reverse reaction.[38] Both options are suitable for producing SAM analogues for the transfer of alternative alkyl groups.[39–42] The inhibiting SAM-derived byproduct SAH (in the case of conventional MTs) can be removed using natural salvage enzymes: either SAH hydrolase (SAHH, E.C. 3.3.1.1),[43] or MTA/ SAH nucleosidase (MTAN, E.C. 3.2.2.16) yielding adenosine or adenine, respectively. MTAN offers the advantages of its broader substrate range and catalysing an irreversible reaction. In biology, MTAN also cleaves the SAM-derived byproducts DOA (from radical SAM enzymes) and MTA (from ACP transfers and polyamine biosynthesis), yielding the corresponding ribose derivative and adenine.[34,44] SAM supply cascades are well established and have been used for many different scenarios;[41,45–51] however, mainly for conventional SAM-dependent MTs, using the physiological cofactor or SAM analogues.[39,48,50] Radical SAM enzymes have been used in combination with MAT or MTAN for the *in situ* production of cofactor (analogues) or the removal of DOA, respectively.[52–55] Nevertheless, depending on the application, a cofactor regeneration system is desired that does not require stoichiometric amounts of the precursors ATP or CldA. For instance, the low amount of cofactor present can simplify downstream processing of the main product.[56] For conventional SAM-dependent MTs a biomimetic cycle using SAHH has been implemented: the resulting adenosine is rephosphorylated to ATP using polyphosphate (polyP) as a phosphate donor. Optionally, the second SAHH product, L-homocysteine, can be remethylated using homocysteine *S*-methyltransferase (E.C. 2.1.1.10) in combination with methylmethionine as a methyl donor, reaching up to 200 total turnover numbers (TTN).[57,58] This system is also applicable for L-Met and nucleobase derivatives. Another approach for SAM regeneration uses the reverse reaction of a halide MT (HMT, E.C. 2.1.1.165) to directly remethylate SAH using methyliodide with up to 500 TTN;[59] this has been expanded to the use of other alkyl halides for general alkylation.[60–63] Both regeneration systems have in common that they rely on SAH formed in the MT reaction. Hence, they can only support MTs since APTs and radical SAM enzymes produce MTA and DOA, respectively. During the development of both systems adenine was identified as a dead-end byproduct that cannot be regenerated in the implemented setups and is consequently lost as a cofactor building block. In the HMT system, this undesired activity was traced back to the co-purified MTAN enzyme from *E. coli*, and could be resolved by using an *mtan*-knockout *E. coli* strain for heterologous expression.[59] For the biomimetic multi-step system this was also partially successful, although a small amount of adenine is additionally formed through a nucleosidase side activity observed for SAHH from *Mus musculus*.[58]

In this work, we used adenine as a starting point for an *in vitro* biomimetic SAM regeneration cycle applicable for all three SAM-derived byproducts: SAH, DOA, and MTA. Such a flexible system has the potential to unlock polyamine synthesis and the vast chemistry of radical SAM

135 enzymes for SAM regeneration. The envisioned regeneration cycle can be split into two parts, one of them being the established SAM supply/SAM-derived byproduct degradation cascade, consisting of a MAT, the SAM-dependent enzyme, and MTAN. In the second part, ATP is regenerated from adenine *via* a ribophosphorylation cascade and further phosphorylation of the resulting AMP to ATP using polyphosphate kinases 2 (PPK2, E.C. 2.7.4.1) (Fig. 2).

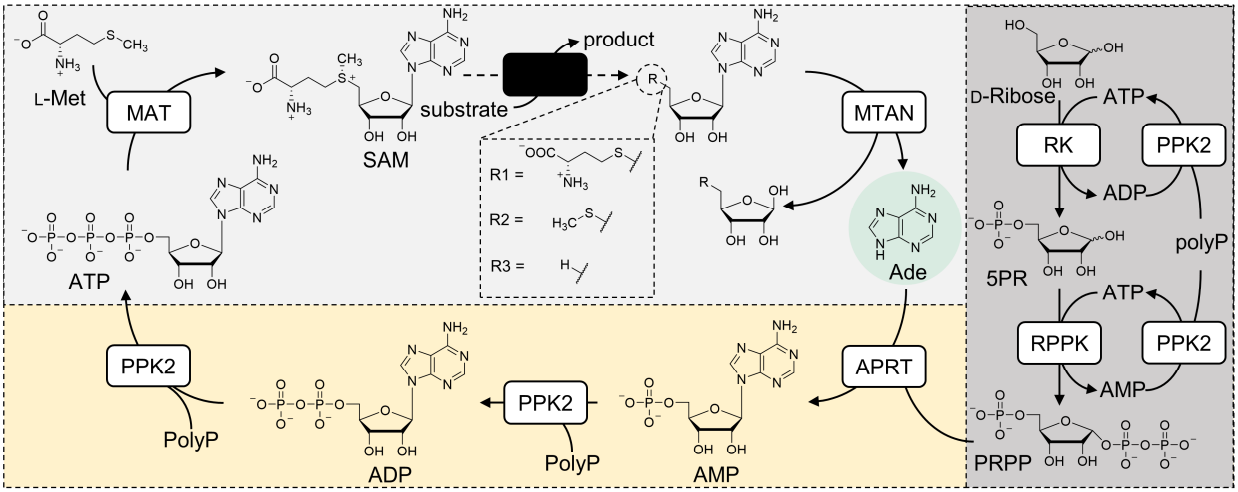

140

Fig. 2 The SAM regeneration system supporting MTs, APTs and radical SAM enzymes envisioned in this work. The system is based on a SAM supply cascade consisting of MAT for SAM supply from L-Met or an analogue, and ATP, SAM-dependent enzyme(s) (black rounded box) and MTAN for byproduct cleavage (light grey). The 5´-residue of the ribosyl moiety depends on the class of SAM-dependent
145 enzymes: R1 for MTs, R2 for APTs and R3 for radical SAM enzymes. The adenine (Ade) produced in the MTAN reaction is the starting point for SAM regeneration by condensing it with 5-phosphoribosyl-1-pyrophosphate (PRPP) synthesised by a ribose phosphorylation cascade (dark grey). The AMP formed is phosphorylated twice to yield ATP, completing the cycle (yellow).

150 **Results**

In situ production of PRPP enables the production of ATP from adenine.

In the natural salvage pathway of nucleotide biosynthesis, ribophosphorylation is carried out by phosphoribosyltransferases using 5-phosphoribosyl-1-pyrophosphate (PRPP) as a cofactor. The use of PRPP introduces new challenges: similarly to SAM, PRPP is an unstable
155 and expensive compound.[64] Consequently, we aimed for a biomimetic *in situ* synthesis of PRPP from D-ribose using ribokinase (RK, E.C. 2.7.1.15) and D-ribose-5-phosphate pyrophosphokinase (RPPK, E.C. 2.7.6.1) (Fig. 2, dark grey box). Similar systems have been successfully used before to produce different types of nucleotides from their corresponding nucleobase.[65,66] Both, RK and RPPK, use ATP for the phosphorylation reactions. Different
160 regeneration systems have been used for the rephosphorylation of ADP (RK reaction) or AMP (RPPK reaction). Based on our prior experience, we chose a set of PPK2 enzymes established in our laboratory: *Aj*PPK2 from *Acinetobacter johnsonii* and *Sm*PPK2 from *Sinorhizobium meliloti* for the polyP-dependent phosphorylation of AMP and ADP, respectively.[57] The ATP

production from adenine, D-ribose and polyP was built up stepwise. First, PRPP production from D-ribose (3 mM) and a catalytic amount of AMP (0.2 mM) was followed by ^{31}P-NMR to ensure that the enzymes are active under the conditions established for SAM supply cascade enzymes (Fig. S2a). The final assay setup contained RK, RPPK and adenine phosphoribosyltransferase (APRT, E.C. 2.4.2.7) from *E. coli*, as well as *Aj*PPK2 and *Sm*PPK2. In addition to D-ribose and adenine (1 mM each), a catalytic amount of ATP (0.2 mM) was used for the RK and RPPK reaction, as well as an excess of polyP for ATP regeneration (Fig. 2, dark grey box). Analysis by HPLC at 254 nm showed that a mixture of the nucleotides AMP, ADP and ATP was formed, while adenine was consumed (Fig. S2b). This is consistent with the expected formation of AMP *via* PRPP catalysed by APRT. The distribution between AMP, ADP and ATP results from the activities of the PPK2 enzymes, which are expected to produce a mixture of nucleotides when both enzymes are present, also due to their adenylate kinase reactivity with the resulting formation of ATP and AMP from ADP and *vice versa*.[67]

Having established the regeneration of ATP from adenine, this could be universally linked with the linear SAM supply/ SAM-derived byproduct degradation cascades (Fig. 2, light grey box) for all three types of SAM-dependent enzymes: conventional MTs, radical SAM enzymes, and APTs. The performance of each enzyme class was first tested in the SAM supply cascade containing MAT and MTAN (Fig. 2, light grey box) and then integrated into the cycle (Fig. 2, light grey, dark grey and yellow box).

SAM regeneration from SAH via adenine/MTAN works with conventional MTs using an S_N2 mechanism.

To demonstrate the incorporation of MTs into the system, we chose anthranilate *N*-MT from *Ruta graveolens* (*Rg*ANMT, E.C. 2.1.1.111) and catechol *O*-MT from *Rattus norvegicus* (*Rn*COMT, E.C. 2.1.1.6) (Fig. 3). These enzymes have been successfully integrated into the linear SAM supply cascade containing MAT and MTAN, as well as the biomimetic SAHH cycle, and are thus a well-suited comparison.[51,57,58] In the linear cascade, *Rn*COMT was investigated for its byproduct inhibition, showing the benefits of MTAN addition.[51] Due to this prior work, the combined regeneration system was set up without first tests of the SAM supply and degradation cascade. The combined regeneration system contained the purified enzymes, starting materials, and salts and was incubated for 20 h. Samples were analysed by HPLC (details in the experimental section). Three different AMP concentrations were tested for each enzyme, corresponding to 10×, 50× and 100× excess of the substrate (2mM) over AMP. As a parameter for the performance of the system, the number of catalytic cycles was determined as the total turnover number (TTN) by the ratio of product formed to added cofactor after 20 h.[68,69]

A 10× excess of substrate compared to AMP led to full conversion and a TTN of 10 with both MTs. A TTN of 46 ± 4 was determined for *Rn*COMT with 50× excess of substrate (Fig. 3a); as

observed before,[58] *Rg*ANMT was less efficient, nevertheless with a conversion of 65% (TTN 33 ± 1, Fig. 3b). The highest TTN measured for this system was 80 ± 5 for *Rn*COMT at 100× substrate excess over AMP (Tab. 1, Fig. S3a).

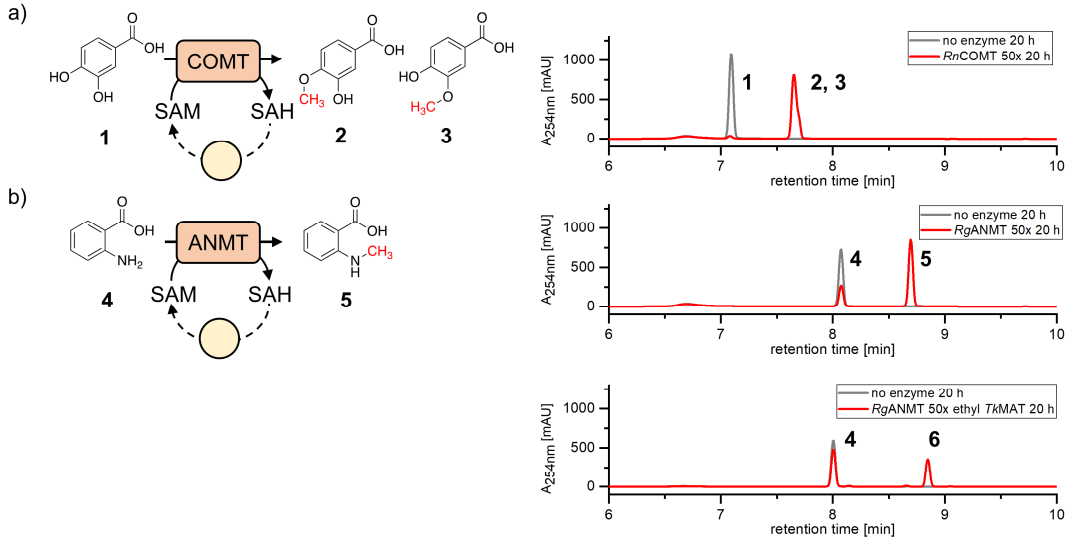

Fig. 3 Reactions and HPLC-analysis of conventional MTs using the SAM regeneration *via* adenine (yellow circle). **a)** 3,4-Dihydroxybenzoic acid (**1**) was methylated to yield a mixture of isovanillic acid (**2**) and vanillic acid (**3**). The chromatogram shows conversion of **1** to a mixture of **2** and **3** after 20 h in experiments containing 50× excess of substrate over AMP compared to a no enzyme control containing (**2** and **3** were not separated by the HPLC method used). **b)** Anthranilic acid (**4**) was converted to *N*-methylanthranilic acid (**5**). Chromatograms are shown for experiments with 50× excess of substrate over AMP with either L-Met (top) or L-Eth (bottom) present. Assays with L-Met showed conversion of **4** to **5**, and assays with L-Eth showed conversion of **4** to *N*-ethylanthranilic (**6**). *Tk*MAT replaced *Ec*MAT in the L-Eth assays.

To investigate the ability of the SAM regeneration system to support alkylation reactions other than methylations, MAT from *Thermococcus kodakarensis* (*Tk*MAT) was used for *S*-adenosylethionine (SAE) generation as the enzyme showed favourable properties towards the acceptance of SAM analogues.[70,71] L-Ethionine (L-Eth) replaced L-Met in these experiments. Otherwise, the assay setup remained the same. *Rg*ANMT was used for ethyl transfer to anthranilic acid for comparison to previous multi enzyme SAM regeneration systems.[57,58] With 50× excess of substrate over AMP, 30% conversion and 15 TTN were observed (Fig. 3b), slightly higher than the previously reported 20% for the adenosine/SAHH-based regeneration system.[57] This supports the assumption that MAT and/or ANMT require higher amounts of cofactor building blocks when L-Eth is used, especially as the corresponding linear cascade showed >75% conversion.[57,58]

SAM regeneration from MTA supports aminopropyl transfer in polyamine synthesis.

After successful SAM regeneration from SAH, the flexibility of the system was investigated by integrating polyamine synthesis. The transfer of the aminopropyl unit in the biosynthesis of polyamines from SAM is a two-step process: first, SAM is decarboxylated by SAM-decarboxylase (SAMDc, E.C. 4.1.1.50). Then, the generated decarboxy-SAM (dcSAM,

S-adenosylmethioninamine) is used as an aminopropyl group donor, with e.g. putrescine attacking dcSAM in an S_N2 reaction as a nucleophile. This polyamine aminopropyltransferase (PAPT) catalysed transfer produces MTA as a byproduct (Fig. 1a).[72] Hence, SAM regeneration from MTA is required (Fig. 4).

As PAPT model enzymes, spermidine synthase (SpeS, E.C. 2.5.1.16) from both *Arabidopsis thaliana* (*At*SpeS isoenzyme 1)[73,74] and *E. coli* (*Ec*SpeS)[72] were selected using putrescine as a substrate. SAMDc from *Thermotoga maritima* (*Tm*SAMDc) was used for the first step of the reaction.[75] For HPLC analysis with detection at 254 nm, the assay samples were derivatised with benzoyl chloride (BzCl).[76]

The envisioned multi-enzyme system was first investigated using a linear SAM supply cascade consisting of *Ec*MAT, *Tm*SAMDc, *At*SpeS (or *Ec*SpeS), and *Ec*MTAN. To avoid derivatisation of Tris, the buffer system was altered to MOPS for all assays containing polyamines. Both, *Ec*SpeS and *At*SpeS showed comparable activity in MOPS and Tris. (Fig. S4a, Fig. S4b). As expected,[77] the removal of inhibitory MTA by addition of MTAN to the experiment accelerated the formation of spermidine. For *Ec*SpeS, addition of MTAN increased the conversion after 1 h by 25%, for *At*SpeS by 16% (Fig. S4c). Interestingly, further aminopropylation of spermidine yielding spermine was detected only in assays with MTAN present after 20 h, supporting the inhibitory character of MTA on SAMDc and/or SpeS. Formation of spermine was observed for both *At*SpeS and *Ec*SpeS (Fig. S4d); while this has been known for *Ec*SpeS, *At*SpeS has previously been reported to lack spermine synthase activity in *in vivo* experiments.[73] In the next step, the ATP production system was added to close the cycle. The performance of the system with SAMDc and SpeS was evaluated after 20 h. Although the system gets more complex through the introduction of another enzyme (SAMDc), the performance was comparable to conventional MTs. Similar conversion rates for both SpeSs were observed, with >94% conversion (putrescine to spermidine and spermine) for a 10× excess of substrate over AMP and conversion of up to 57% for 100× excess of substrate (Tab. 1, Fig. 4, Fig S4d). Conversion to spermine was only observed for samples with 0.2 mM AMP, suggesting that a high level of spermidine must be available as substrate for spermine synthesis (Fig. S4d).

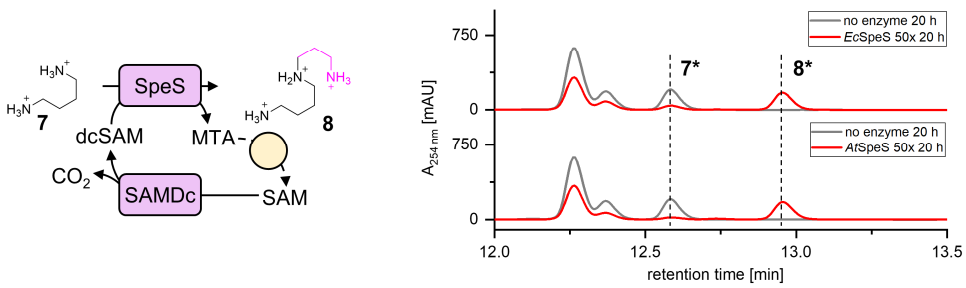

Fig. 4 The SAM regeneration system with APTs. Spermidine synthase (SpeS) alongside SAM decarboxylase (SAMDc) was utilised as a model enzyme for aminopropyl transfer from dcSAM to putrescine (**7**) yielding spermidine (**8**). The SAM regeneration system is indicated by the yellow circle.

The top chromatogram shows conversion for *Ec*SpeS, the bottom chromatogram shows conversion for
265 *At*SpeS, both at 50× excess of substrate over AMP. All peaks correspond to the BzCl-derivatised polyamines (*).

The SAM regeneration system supports class B radical SAM MTs by SAM regeneration from SAH and DOA.

270 For the incorporation of radical SAM enzymes, the cobalamin-dependent glutamine *C*-MT (QCMT) from *Methanoculleus thermophilus* was selected as a model enzyme. This recently described enzyme is involved in the posttranslational modification of methyl-coenzyme M reductase where it catalyses the methylation of the sp^3-C2 of Q418 (Fig. 5a).[52] This enzyme requires two SAM molecules per catalytic cycle: one is homolytically cleaved into L-Met and a
275 DOA• radical, the other serves as a methyl group donor to Co(I) of bound cobalamin to generate methylcobalamin (MeCbl(III)) under release of SAH. The DOA• radical then abstracts a hydrogen atom from C2 of the glutamine residue, resulting in DOA and the corresponding peptidyl radical. The methylation of the peptidyl radical proceeds via homolytic cleavage of the cobalt-carbon bond producing the methylated peptide and cob(II)alamin (Cbl(II), Fig. 5a).[52]
280 As both, DOA and SAH, are substrates for MTAN[34], the regeneration system should be capable of cleaving both byproducts (SAH and DOA) and regenerating two equivalents of SAM from adenine per methylation reaction.

Initially, the three-enzyme methylation cascade was modified to incorporate radical SAM enzymes. Reactions were performed in an anoxic chamber, and the buffer was complemented
285 with 300 mM NaCl to ensure enzyme stability. Also, 1 mM Ti(III)citrate was added to the assays as a reducing agent. Ti^{3+} has been shown to reduce the $[4Fe4S]^{2+}$-cluster into the required $[4Fe4S]^{1+}$ oxidation state as well as the cob(II)alamin into the cob(I)alamin state, and is therefore a well-suited reductant for class B radical SAM MTs.[52,78] Adding cobalamin to the assay mixture was not necessary as the enzyme was reconstituted with hydroxocobalamin
290 after purification, which remains tightly bound to the enzyme.[52] A 24-mer peptide fragment of methyl-coenzyme M reductase was used as the substrate as described previously.[52] Analysis of the linear cascade consisting of MAT, QCMT, and MTAN by liquid chromatography mass spectrometry (LC-MS) revealed full conversion after 20 h (Fig. S5a). In the next step, QCMT was coupled to the full SAM regeneration system, initially with a 10× excess of substrate over
295 AMP (0.4 mM and 0.04 mM, respectively), corresponding to 20 possible TTN of the regeneration system as two SAM molecules are required for one methyl transfer to the peptide. After 20 h, analysis by LC-MS showed a conversion of 90% ± 3%, corresponding to a TTN of 18 ± 1 (Fig. S5b).

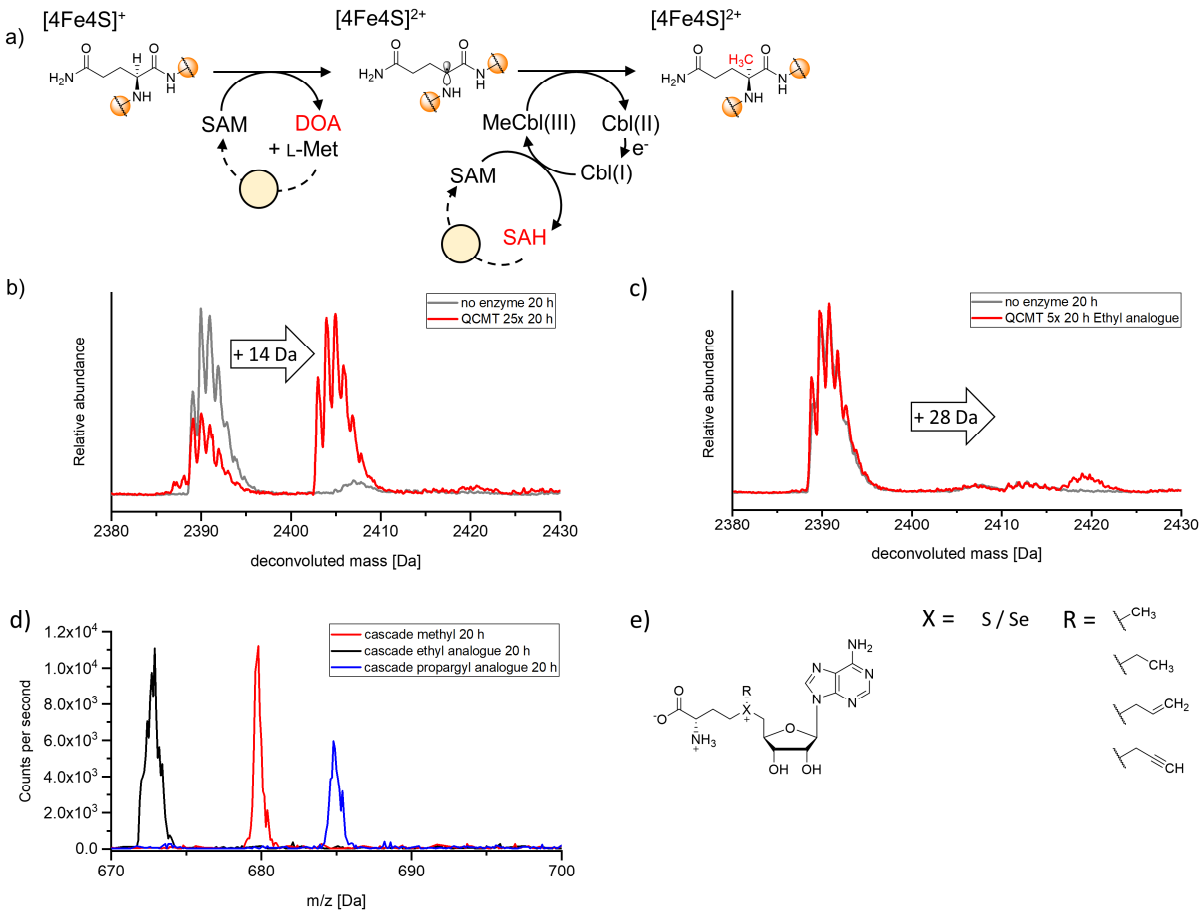

f)

Analogue	DOA	SAH/*Se*AH	Alkyl Cobalamin	Peptide alkylation
Ethyl	Yes	Yes	Yes	Yes
Allyl	No	Yes	No	No
Se-propargyl	Traces	Yes	Yes	No
Se-methyl	Yes	Yes	n. d.	Yes

Fig. 5 SAM regeneration for class B radical SAM MTs. **a)** QCMT methylates C2 of a glutamine residue within a peptide chain (orange) under retention of stereochemistry.[52] Two SAM molecules are utilised, one for radical generation, the other for cobalamin methylation. DOA and SAH are formed as byproducts, both can be regenerated to SAM (yellow circle). **b)** LC-MS analysis of assays with 25× excess of peptide substrate (m = 2390.1 Da) over AMP (50 theoretical TTN) showed a mass shift of +14 Da (m = 2404.1 Da), consistent with methylation. **c)** Usage of L-Eth instead of L-Met in the SAM regeneration system with 5× excess of peptide substrate over AMP leads to ethylation of the peptide substrate, indicated by a mass shift of +28 Da (m = 2419.0 Da). **d)** Analysis of cobalamin bound to the enzyme shows evidence for methyl- (m/z 672.9 Da), ethyl- (m/z 679.8 Da) and propargylcobalamin (m/z 684.8 Da) in cascade assays with the respective SAM analogue present. Each cobalamin species was detected as m + 2 H^+. **e)** Analogues of SAM tested with QCMT. **f)** Overview of the observed species in QCMT assays using the individual L-Met analogues.

In experiments with 25× excess of peptide over AMP (in theory allowing a TTN of 50), an average conversion of 56% ± 22% was reached, amounting to 28 ± 11 TTN. (Fig. 5b) This is less than for MTs and APTs, and might be related to the lower amounts of AMP (0.02 mM vs. 0.04 mM) used due to low concentration of peptide substrate.

Tab. 1 Combined quantitative data for the SAM regeneration system *via* MTAN/Ade.

Enzyme	c(AMP) [mM]	substrate excess	conversion [%]	TTN
*Rn*COMT	0.2	10×	100 ± 0	10 ± 0
	0.04	50×	93 ± 9	46 ± 4
	0.02	100×	80 ± 5	80 ± 5
*Rg*ANMT	0.2	10×	97 ± 3	10 ± 0
	0.04	50×	65 ± 1	33 ± 1
	0.02	100×	67 ± 12	67 ± 12
*Ec*SpeS	0.2	10×	96 ± 1	10 ± 0
	0.04	50×	82 ± 4	41 ± 2
	0.02	100×	57 ± 10	57 ± 10
*At*SpeS	0.2	10×	98 ± 0	10 ± 0
	0.04	50×	79 ± 8	40 ± 4
	0.02	100×	55 ± 11	55 ± 11
QCMT	0.04	10×	90 ± 3	18 ± 1
	0.02	25×	56 ± 22	28 ± 11

Since some conventional MTs are able to transfer alternative alkyl chains such as ethyl (from L-Eth/SAE), we wondered if QCMT would be able to generally catalyse alkyl transfer to the peptide substrate. Such an activity by class B radical SAM MTs would be highly interesting, as it would potentially enable the stereo- and regioselective introduction of new functionalities to unactivated sp^3 carbons. These modified products would also be useful tools in mechanistic studies on different types of radical SAM enzymes. Nevertheless, the SAM analogue would have to support the generation of the DOA• radical and the corresponding alkylcobalamin. In addition, the alkylcobalamin must be able to react with the substrate radical. The ability to generate the DOA• radical from SAM analogues has been previously demonstrated for *Se*-adenosyl selenomethionine (*Se*SAM), SAE, *S*-adenosyl allylhomocysteine, nucleobase analogues, and the sulfoxide derivative of SAH.[79–83] Alkylcobalamins other than MeCbl and AdoCbl have only been produced by preparative synthetic methods.[84]

We investigated the three enzyme cascade consisting of MAT, QCMT and MTAN with L-Eth, D,L-allylhomocysteine and L-propargylselenohomocysteine instead of L-Met, using the *Methanocaldococcus jannaschii* MAT variant L147A/I351A (PC*Mj*MAT) optimised for the formation of SAM-analogues with bulkier residues (Fig. 5e).[85] Analysis by LC-MS of the L-Eth assay showed a signal at 2419.0 Da, corresponding to a mass shift of +28 Da, thereby supporting ethylation of the peptide. In addition, assays containing no MTAN showed peptide

ethylation with SAH and DOA formation (Fig. 5f, Fig. S5c). Further analysis of the cobalamin bound to the enzyme by LC-MS revealed a species with the m/z of 679.8 Da, corresponding to ethylcobalamin + 2 H^+. Neither allylation, nor propargylation of the peptide was observed. When looking for the corresponding alkylcobalamins, propargylcobalamin + 2 H^+ could be detected at an m/z of 684.8 Da (Fig. 5d), however no allylcobalamin. Analysis of the propargylation assays containing no MTAN revealed a peak likely corresponding to the seleno-analogue of SAH (*Se*SAH), while only trace amounts of DOA could be observed in the chromatogram. Interestingly, even though no allylcobalamin was detected, SAH was observed in the assay with the allyl analogue (Fig. 5f; Fig. S5c). The lack of DOA formation for both, the allyl and propargyl analogue, suggests that either these analogues are not able to support radical generation due to sterical restrains, or that the *S/Se*-alkyl bond is cleaved rather than the *S/Se*-C5′ bond. The latter could be supported by the π-system of these analogues, as it makes the *S/Se*-alkyl bond the weakest bond. However, experiments with allyl-SAM and NosN resulted in functional enzyme with cleavage of the S-C5′ bond.[81] In addition, photoinduced cleavage of SAM bound to HydG or PFL-AE suggests that regioselectivity of bond cleavage is determined by the geometry of SAM bound to the [4Fe4S]-cluster.[86] Hence, the bulkier residues would have to alter the binding of SAM to allow cleavage of the S/Se-alkyl bond. Interestingly, the expected C-alkyl bond cleavage byproduct (Se)SAH is formed with all tested analogues. However, it is also the byproduct of cobalamin alkylation and therefore an expected byproduct for the enzyme. The lack of allylcobalamin can be explained with rapid degradation by homolytic cleavage of the allyl-Co bond under formation of a stable allyl radical and cob(II)alamin (Fig. S5e).

To investigate if the *Se-C*-bond hinders the formation of the DOA• radical in the propargylation assays, L-selenomethionine was used to yield *Se*SAM. Methylation of the peptide indicated a fully functional enzyme. As HPLC analysis confirmed the formation of DOA (Fig. S5c), we concluded that the *Se-C*-bond was not impeding the radical formation.

Finally, we investigated whether the SAM regeneration system was able to support ethylation of the peptide substrate. L-Met was replaced with L-Eth and the peptide substrate was present in 5× excess. After 20 h, a portion of approximately 7% ethylated product was detected (Fig. 5c), which was in the same range as the conversion obtained for the linear cascade (~14%, Fig. S5d).

Discussion

In situ synthesis and regeneration of SAM are important steps towards the efficient utilisation of the cofactor for biocatalytic applications. However, all SAM regeneration systems designed so far have been limited to SAH producing MTs.[57–59] The SAM regeneration system presented

375 in this work unlocks the full potential of the highly versatile cofactor SAM, including radical SAM enzymes and polyamine synthases. This is achieved by regenerating SAM *via* the former dead-end byproduct adenine using cheap and stable starting material and catalytic amounts of AMP. As SAH, MTA and DOA have been shown to be potential inhibitors for SAM-dependent enzymes[35,53,77], their removal and regeneration represent a valuable tool to
380 increase the activity of SAM-dependent enzymes for synthetic and mechanistic studies. Especially the incorporation of radical SAM enzymes is promising for future applications due to their vast chemical capabilities. Particularly in drug synthesis the ever expanding chemical space of radical SAM enzymes can be useful for challenging reactions, e. g. stereo- and regioselective methylation of non-activated carbons.
385 The supply and regeneration systems are also able to support *in situ* synthesis of alkyl analogues and alkyl transfer. This opens up the possibility of directly introducing desired functional groups stereo- and regioselectively to unactivated sp^3 carbon atoms enzymatically. In addition to the possibility of enhancing the diversity of radical SAM MT products by transferring alternative alkyl chains, this might be interesting in terms of using SAM analogues
390 for mechanistic studies as has been shown before.[79–81,83] Building up the SAM molecule from the basic building blocks nucleobase, sugar, phosphates, and alkylated homocysteine gives full flexibility for all types of SAM analogues.[45,87] Although first attempts to introduce allyl- or propargyl residues to the substrate were unsuccessful, the system seems flexible towards alkyl analogues, as we showed using SAE. Together with the increasing number of solved enzyme
395 structures, it might be possible to design enzyme variants with a broader or altered substrate range, as has been shown for MATs and conventional MTs.[85,88–90]

In summary, our flexible SAM regeneration system using adenine as a central building block represents a promising tool to improve turnover rates, attenuate byproduct inhibition issues as well as increase mechanistic understanding and biocatalytic applications of SAM-dependent
400 enzymes including radical SAM enzymes in the future.

Methods

Materials & Reagents

All chemicals were purchased in the highest purity available from Sigma-Aldrich (ATP, ADP, AMP, SAM, SAH, MTA, L-methionine, L-ethionine, L-selenomethionine, *N*-ethylanthranilic acid, 3,4-dihydroxybenzoic acid, putrescine, spermidine, spermine), Acros Organics (isovanillic acid and sodium polyphosphate), Alfa Aesar (*N*-methylanthranilic acid, vanillic acid), AppliChem (adenine) and Fluka (anthranilic acid). Ingredients for buffers and cultivation media were purchased from Carl Roth. The peptide substrate for QCMT (*H*-PTMMEDHFGGSQRAGVIAAASGLS-*OH*) was purchased at TAG Copenhagen (Denmark).

Protein Production

The genes encoding ribokinase (RK) and adenosine phosphoribosyltransferase (APRT) were amplified from *E. coli* genomic DNA by PCR using the primers given in Tab. 2 and cloned into pET28a using T4 DNA ligase (New England Biolabs GmbH, Germany). The gene encoding ribose-phosphate pyrophosphokinase (RPPK) was also amplified from genomic DNA of *E. coli* and cloned into pET28a using In-Fusion cloning (Takara Bio Europe, France).

Tab. 2 PCR primers used in this study. Restriction sites are shown in bold.

Primer	Sequence (5' → 3')
ecrk_for	GCGGCAGC**CATATG**ATGCAAAACGCAGGCAGCC
ecrk_rev	GCGGCCGC**AAGCTT**TCACCTCTGCCTGTCTAAAAATGCG
ecaprt_for	GCGGCAGC**CATATG**ATGACCGCGACTGCACAGC
ecaprt_rev	TGGTGGTG**CTCGAG**TTAATGGCCCGGGAACGG
ecrppk_for	CGCGCGGCAGC**CATATG**CCGGATATGAACC
ecrppk_rev	GTGCGGCCGC**AAGCTT**AATGTTCAAACATC

QCMT was produced and purified as described previously.[52] All other enzymes were produced as follows: *E. coli* BL21-Gold(DE3) (Agilent, Santa Clara, USA) cells transformed with the respective pET28a construct were grown in lysogeny broth (LB) medium supplemented with kanamycin (50 µg/mL) at 37 °C with shaking until an OD_{600} of 0.5-0.6 was reached. Gene expression was induced by addition of 0.2 mM of isopropyl β-D-1-thiogalactopyranoside (IPTG) and cultures were further incubated overnight at 20 °C. The harvested cell pellet was resuspended in lysis buffer [40 mM Tris-HCl, pH 8.0, 100 mM NaCl, 10% (*w*/*v*) glycerol] and lysed by sonication (Branson Sonifier 250, Emerson, USA) The

lysates were used for protein purification by Ni(II)-NTA affinity chromatography (Invitrogen, Thermo Fisher Scientific, USA) as previously described.[58] Desalting was carried out using a PD-10 column (GE Healthcare Life Sciences, UK). For PC*Mj*MAT the protein was further purified by heating at 80 °C for 20 min followed by 30 min centrifugation at 18213 × g (Eppendorf centrifuge 5427 R). Protein concentrations were determined by UV/vis absorption with calculated extinction coefficients (ε_{280}, ExPASy ProtParam)[91] using a NanoDrop 2000 (Thermo Fisher Scientific, USA). Purity of the enzymes was assessed by SDS-PAGE[92] (Fig. S1).

Synthesis of methionine analogues

Allyl-D,L-homocysteine

As described previously[93], D,L-homocysteine (100 mg, 0.74 mmol, 1 eq.) was dissolved in 2 mL of H_2O and 124 mg of $NaHCO_3$ (1.48 mmol, 2 eq.) were added. To this solution 115 µL of allyl bromide (1.34 mmol, 1.8 eq.) was added and the mixture was stirred for 3 h at 40 °C. The reaction was cooled to room temperature, adjusted to pH = 3 with 1 M HCl and purified via preparative HPLC. The product was obtained as white crystalline solid (56 mg, 0.32 mmol, 43 %). The identity was confirmed by HRMS (LTQ Orbitrap XL**,** Thermo Fisher Scientific, Fig. S6), ^{1}H NMR and ^{13}C NMR (Fig. S7).

^{1}H NMR (400 MHz, D_2O + 1 % NaOD) δ (ppm) = 5.82 (m, 1H), 5.31 – 5.10 (m, 2H), 3.30 (m, 1H), 3.20 (m, 2H), 2.53 (m, 2H), 1.98 – 1.67 (m, 2H).

^{13}C-{^{1}H}-NMR (101 MHz, D_2O + 1 % NaOD) δ (ppm) = 182.8, 134.0, 117.6, 55.3, 34.4, 33.5, 26.3.

Propargyl-L-selenohomocysteine

First, L-selenohomocysteine was synthesized in two steps starting from L-homoserine (Activate Scientific) as previously reported by Bothwell *et al.*.[94] Under an argon atmosphere L-selenohomocysteine (119 mg, 0.65 mmol, 1 eq.) was dissolved in 20 mL dry ethanol. Sodium borohydride (124 mg, 3.28 mmol, 5 eq.) was added and the mixture was stirred for 15 min at room temperature. Sodium bicarbonate (150 mg, 1.78 mmol) and propargyl bromide (80 % in toluene, 156 µL, 208 mg, 1.26 mmol, 2 eq.) were added and the mixture stirred for 16 h. The solvent was removed under reduced pressure. The raw product was dissolved in 240 mM HCl (10 mL) and purified *via* preparative HPLC. The product was obtained as white crystalline solid (100mg, 0.45 mmol, 69 %). The identity was confirmed by HRMS (LTQ Orbitrap XL**,** Thermo Fisher Scientific, Fig. S8), ^{1}H NMR and ^{13}C NMR (Fig. S9).

^{1}H NMR (400 MHz, D_2O) δ (ppm) = 3.84 (t, *J* = 6.9, 5.6 Hz, 1H), 3.39 – 3.28 (m, 2H), 2.92 – 2.82 (m, 2H), 2.67 (t, *J* = 2.7 Hz, 1H), 2.38 – 2.19 (m, 2H).

^{13}C-{^{1}H}-NMR (101 MHz, D_2O) δ (ppm) = 171.8, 79.2, 69.9, 52.5, 28.9, 16.7, 4.2.

470

Enzyme assays

In general, all enzyme assays were at least performed in triplicates. If not stated differently, negative controls contained no enzyme.

475 Ribose phosphorylation

Initial assays investigating the phosphorylation of ribose towards PRPP were set up with *Ec*RK, *Mycobacterium tuberculosis* RPPK (*Mt*RPPK)[95], *Sm*PPK2 and *Aj*PPK2 with an excess of polyphosphate (polyP) and catalytic amounts of AMP. The assay composition was as follows: 50 mM Tris buffer pH 7.5, 50 mM KCl, 20 mM $MgCl_2$, 30 mM polyP, 3 mM D-ribose, 0.03 µM
480 *Ec*RK, 2 µM *Mt*RPPK, 1 µM *Aj*PPK2 and 1 µM *Sm*PPK2. D_2O was added to a final concentration of 10% and 0.5 mM cAMP was added as an internal standard. The assays were started by addition of 0.2 mM AMP. PRPP production was followed by ^{31}P NMR on a Bruker (Billerica, USA) Avance Neo 400 MHz spectrometer at 162 Mhz with a 5 mm BB Prodigy probehead. The sample was tempered to 37 °C without agitation. The spectrum of the last data point was
485 manually phased, the resulting parameters were applied to all other datasets. PRPP concentration was determined by integration of the anomeric-bound pyrophosphate unit with signals at -11.5 ppm (α-phosphate), at -5.80 to -5.86 ppm (terminal β-phosphate) and at 3.27 to 2.87 ppm (5'-phosphate). D-Ribose-5-phosphate concentration was determined by integration of signals shifted from 3.28 ppm to 2.87 ppm.

490 Assays investigating the nucleotide production from D-ribose were carried out as follows: 50 mM KP_i buffer (pH 7.5), 50 mM KCl, 20 mM $MgCl_2$, 1 mM adenine, 1 mM D-ribose, 20 mM polyP, 2.9 µM *Ec*RK, 2.7 µM *Mt*RPPK, 4.5 µM *Ec*APRT, 0.9 µM *Aj*PPK2, 1.4 µM *Sm*PPK2 and 0.2 mM ATP were added to a final volume of 1 mL and incubated for 1 h at 37 °C without agitation. Samples were taken at 0 min, 15 min, 30 min, and 60 min and snap frozen in liquid nitrogen.
495 For HPLC analysis the samples were centrifuged for 20 min at 4 °C, 18213 × g (Eppendorf centrifuge 5427 R) and the supernatant was filtered using Vivaspin® 500 Centrifugal Concentrators (10,000 MWCO, Sartorius AG, Germany). Samples were analysed using HPLC method A.

500 Methyl Transferase Assays

The assays for SAM regeneration were carried out in a reaction mixture (400 µl) with final concentrations of 50 mM Tris buffer (pH 7.5) with 20 mM $MgCl_2$, 50 mM KCl and 20 mM polyP. The substrates for the methylation reactions, either anthranilic acid or 3,4-dihydroxybenzoic acid, were added to the final concentration of 2 mM. D-ribose and L-methionine (L-Met) were
505 added in slight excess at 3 mM. For ethylation assays, L-ethionine (L-Eth) was used instead of L-Met (also 3 mM). The enzymes were used at the following final concentrations: 3 µM *Ec*RK, 3 µM *Ec*RPPK, 3 µM *Ec*APRT, 1 µM *Aj*PPK2, 1 µM *Sm*PPK2, 10 µM *Ec*MAT and 1 µM of

*Ec*MTAN. Either 10 µM *Rn*COMT or 10 µM *Rg*ANMT. For ethylation assays, *Ec*MAT was replaced with *Tk*MAT. Varying final concentrations (0.2 mM, 0.04 mM and 0.02 mM) of the cofactor building block AMP were added to achieve maximum possible turnover numbers of 10, 50 and 100, respectively. The reaction mixtures were incubated at 37 °C, 350 rpm for 20 h. The reaction was quenched by the addition of $HClO_4$ to a final concentration of 2% and samples were snap frozen in liquid nitrogen. Samples for HPLC analysis were prepared as described above and analysed by HPLC method B.

Spermidine Synthase Assays

Prior to all assays, *Tm*SAMDc was activated by heating at 80 °C for 1 h.[75] Initial polyamine synthesis assays were set up in the linear SAM supply cascade containing MAT and MTAN. 50 mM MOPS, Tris or HEPES buffer pH 7.5, 50 mM KCl, 20 mM $MgCl_2$, 3 mM L-Met, 3 mM ATP, 2 mM putrescine, 10 µM *Ec*MAT, 1.5 µM *Ec*MTAN, 20 µM SpeS and 40 µM *Tm*SAMDc were added to a final volume of 500 µL. The assays were incubated for 20 h at 37 °C.

Polyamine synthesis in the SAM regeneration system was set up as described above for ANMT and COMT with the following alterations: The buffer was 50 mM MOPS pH 7.5 and the MT was replaced by 40 µM *Tm*SAMDc and 20 µM SpeS (*Ec*SpeS or *At*SpeS).

For all SpeS assays, samples were immediately snap frozen in liquid nitrogen without prior quenching and stored at -20 °C until further preparation. The frozen samples were centrifuged at 4 °C at 18213 × g until thawed. 20 µL of the supernatant was used for sample preparation. 20 µL NaOH (0.2 M) and 20 µL benzoyl chloride (40 mM) were added to the sample prior to incubation at 25 °C, 350 rpm for 30 min. The derivatisation reaction was quenched by the addition of 60 µL formic acid (2.5%). Standards for qualitative and quantitative analysis were derivatised accordingly. The derivatised samples were prepared for HPLC analysis (Method C) by centrifugation at 4 °C, 18213 × g for 45 min.

Class B radical SAM MT Assays

All assays containing QCMT were conducted under strict exclusion of oxygen in a Coy anaerobic chamber maintained at 97.5% N_2 and 2.5% H_2. Except for the enzymatic preparations, peptide and Ti(III)citrate, the stock solutions for all other reaction components were prepared freshly inside the anaerobic chamber.

Assays using the linear SAM supply cascade contained 50 mM Tris buffer (pH 7.5) supplemented with 300 mM NaCl, 20 mM $MgCl_2$ and 50 mM KCl. In addition, 1 mM Ti(III)citrate, 0.05 mM peptide (24mer, *H*-PTMMEDHFGGSQRAGVIAAASGLS-*OH*), 2 mM L-Met and 2 mM ATP were added. For the methylation cascade 10 µM *Ec*MAT, 10 µM QCMT and 1 µM *Ec*MAT were used. For assays containing methionine analogues, L-Met was replaced with either 3 mM L-selenomethionine, 3 mM L-Eth, 6 mM D/L-allylhomocysteine or 3 mM

545 L-propargylselenohomocysteine and 50 µM PC*Mj*MAT replaced *Ec*MAT.[96] Assays without *Ec*MTAN were conducted for the analysis of SAH and DOA. All assays were incubated for 20 h at 350 rpm, 37 °C. Samples for peptide, SAH and DOA analysis were quenched by addition of $HClO_4$ at a final concentration of 2.5%. The vials were immediately snap-frozen and stored at -20 °C until use. For LC-MS analysis, the samples were thawed on ice and centrifuged
550 (18213 × *g*, 20 min, 4 °C). The supernatant was passed through a syringe filter (0.2 µm cut-off) and the flow-through obtained was used for LC-MS analysis. Samples for the analysis of cobalamin bound to the enzyme were prepared as previously described.[52]

Assays for investigating the SAM regeneration system with QCMT were carried out in 50 mM Tris buffer (pH 7.5) containing 300 mM NaCl, 20 mM $MgCl_2$ and 50 mM KCl. To this, L-Met,
555 D-ribose, and polyP were added in excess at 3 mM, 3 mM and 20 mM, respectively. Peptide (24mer) was added at 0.5 mM and Ti(III)citrate at 2 mM of final concentration. *Ec*RK, *Ec*RPPK, *Ec*APRT, *Sm*PPK2, *Aj*PPK2, *Ec*MAT and *Ec*MTAN were added as described above. The reaction mixtures were incubated at 37 °C, 350 rpm for 20 h. Assays containing L-Met analogues were altered as described above for the linear cascade. The samples were
560 prepared for LC-MS analysis as described above.

HPLC analysis

Method A: Analysis of samples from assays investigating the formation of nucleotides from D-ribose and adenine was conducted by a reversed phase HPLC method adapted from LIU *et*
565 *al*.[97] An Agilent Technologies 1260 infinity II HPLC system with an ISAspher 100-5 C18 column (250 mm × 4.0 mm, 5 µm, ISERA GmbH, Germany) was used. The temperature of the column was held at 25 °C. The elution gradient was a mixture of two solvents: 100 mM KP_i buffer at pH 7.0 (A) and CH_3CN (B). Following gradient was applied: 0-3 min 0% B, 3-5 min 0% to 5% B, 5-7 min 5% to 20% B, 7-8.3 min 20% to 25% B, 8.3-9 min 25% to 0% B and
570 9-15 min 0% B. The sample injection volume was 10 µL and the flow rate throughout the 15 min run was 1.2 mL/min. Detection of analytes was performed at 254 nm. Retention times of standards are given in Tab. 3.

Tab. 3 Retention times of standards determined for HPLC method A.

Substance	**Retention time [min.]**
Adenine	9.0
ADP	7.7
AMP	8.0
ATP	6.7

575

Method B: Analysis of substrates and products of methyltransferase reactions was carried out on an Agilent Technologies 1260 infinity II HPLC system using ISAspher 100-5 C18 column (125 mm × 4.0 mm, 3 µm, ISERA GmbH, Germany) using a mobile phase of (A) 0.1% formic acid in H_2O and (B) 100% CH_3CN at a flow rate of 1 mL/min. The column was equilibrated with 3% solvent B and after injection of 10 µL of sample, solvent B was applied with a following gradient: 0-4 min 3% B, 4-7 min 3% to 70% B, 7-7.10 min 70% to 100% B, 7.10-10 min 100% B, 10-11 min 100% to 3% B, 11-14 min 3% B. Detection of substrates and methylated products was performed at 254 nm with a diode array detector (DAD). Quantitative determination of substrates and products was carried out by recording calibration curves using authentic references of the following substrates and methylated products: anthranilic acid, 3,4-dihydroxybenzoic acid, *N*-methylanthranilic acid, *N*-ethylanthranilic acid, vanillic acid and isovanillic acid. The retention times and calibration curve equations are given in Tab. 4.

Tab. 4 Retention times of standards determined for HPLC method B.

Substance	**Retention time [min.]**	**Calibration curve**	**R^2**
3-4-dihydroxybenzoic acid	7.1	y = 2032.9x	0.99
Vanillic acid, isovanillic acid	7.6	y = 2388.1x	0.95
Anthranilic acid	8.0	y = 1250.1x	0.99
N-Methylanthranilic acid	8.7	y = 1990.8x	0.98
N-Ethylanthranilic acid	8.9	y = 2151.6x	0.99

Method C: Derivatised polyamine samples were analysed by reversed phase HPLC on an Agilent 1100 Series with an ISAsphere 100-5-C18 column (250 mm × 4.0 mm, 5 µm, ISERA GmbH, Germany). Mobile Phase A was water with 1% CH_3CN and 0.1% formic acid, mobile phase B was CH_3CN. The following gradient was applied at a flow rate of 1.0 mL/min: 0-1.5 min 2% B, 1.5-8 min 2% to 33% B, 8-11 min 33% to 95% B, 11-15.5 min 95% B, 15.5-17.5 min 95% to 2% B, 17.5-22 min 2% B. Injection volume was 10 µL. Peaks were detected at 254 nm by DAD. The retention times an calibration curves are given in Tab. 5.

Tab. 5 Retention times of standards determined for HPLC method C.

Substance	**Retention time [min.]**	**Calibration curve**	**R^2**
Benzoic acid	9.0	n. d.	n. d.
Putrescine*	12.6	y = 450.44x	>0.99
Spermidine*	13.0	y = 529.18x	>0.99
Spermine*	13.2	y = 599.99x	>0.99

Tris*	12.8	n. d.	n. d.

Method D: Analysis of QCMT reaction byproducts was conducted by reversed phase HPLC on an Agilent Technologies 1260 infinity II HPLC system with an ISAspher 100-5 C18 column (250 mm × 4.0 mm, 5 µm, ISERA GmbH, Germany). Mobile phase A was 40 mM Na acetatae buffer pH 4.2, mobile phase B was CH_3CN. The gradient was set up as follows at a flow rate of 0.5 mL/min: 0-16 min 2% B to 30% B, 16-18 min 30% B, 18-20 min 30% to 2% B, 20-30 min 2% B. Injection volume was 10 µL, peaks were detected using a DAD at 260 nm. Retention times of standards are given in Tab. 6.

Tab. 6 Retention times of standards determined for HPLC method D.

Substance	**Retention time [min.]**
Adenine	13.1
ADP	9.0
AMP	11.4
ATP	6.2
DOA	16.6
MTA	19.4
SAH	13.7
SAM	10.8

LC-MS Analysis

Peptide Analysis

Analysis of the 24mer peptide was conducted as previously described.[52] Quantitative peptide turnover measurements were performed with the UniDec Software using the interpolate function.[98] Masses were calculated and measured as average isotopic masses when not stated different.

Cobalamin analysis

Analysis by LC-MS of cobalamin bound to QCMT was conducted as previously described.[52] Masses were calculated and measured as average isotopic masses when not stated different.

Data Availability

All data discussed in this study is available in the main text and in the supplementary information.

References

[1] D. K. Liscombe, G. V. Louie, J. P. Noel, *Nat. Prod. Rep.* **2012**, *29*, 1238–1250.
[2] M. Fontecave, M. Atta, E. Mulliez, *Trends Biochem. Sci.* **2004**, *29*, 243–249.
[3] W. A. Loenen, *Biochem. Soc. Trans.* **2006**, *34*, 330–333.
[4] J. W. Locasale, *Nat. Rev. Cancer* **2013**, *13*, 572–583.
[5] A. E. Morellato, C. Umansky, L. B. Pontel, *Redox Biol.* **2021**, *40*, 101850.
[6] E. J. Barreiro, A. E. Kümmerle, C. A. M. Fraga, *Chem. Rev.* **2011**, *111*, 5215–5246.
[7] H. Schönherr, T. Cernak, *Angew. Chem. Int. Ed.* **2013**, *52*, 12256–12267.
[8] A.-W. Struck, M. L. Thompson, L. S. Wong, J. Micklefield, *ChemBioChem* **2012**, *13*, 2642–2655.
[9] S. Roje, *Phytochemistry* **2006**, *67*, 1686–1698.
[10] H. Lin, *Bioorg. Chem.* **2011**, *39*, 161–170.
[11] Z. Cui, J. Overbay, X. Wang, X. Liu, Y. Zhang, M. Bhardwaj, A. Lemke, D. Wiegmann, G. Niro, J. S. Thorson, C. Ducho, S. G. Van Lanen, *Nat. Chem. Biol.* **2020**, *16*, 904–911.
[12] M. Umitsu, H. Nishimasu, A. Noma, T. Suzuki, R. Ishitani, O. Nureki, *Proc. Natl. Acad. Sci. U.S.A.* **2009**, *106*, 15616–15621.
[13] A. K. Handa, T. Fatima, A. K. Mattoo, *Front. Chem.* **2018**, *6*.
[14] A. J. Michael, *J. Biol. Chem.* **2018**, *293*, 18693–18701.
[15] S. Bienz, P. Bisegger, A. Guggisberg, M. Hesse, *Nat. Prod. Rep.* **2005**, *22*, 647–658.
[16] T. Shoji, T. Hashimoto, in *Polyamines: A Universal Molecular Nexus for Growth, Survival, and Specialized Metabolism* (Eds.: T. Kusano, H. Suzuki), Springer Japan, Tokyo, **2015**, pp. 189–200.
[17] H. J. Sofia, G. Chen, B. G. Hetzler, J. F. Reyes-Spindola, N. E. Miller, *Nucleic Acids Res.* **2001**, *29*, 1097–1106.
[18] J. B. Broderick, B. R. Duffus, K. S. Duschene, E. M. Shepard, *Chem. Rev.* **2014**, *114*, 4229–4317.
[19] Y. Nicolet, *Nat. Catal.* **2020**, *3*, 337–350.
[20] Q. Sun, M. Huang, Y. Wei, *Acta Pharm. Sin. B.* **2020**, *11*, 632–650.
[21] A. Benjdia, C. Balty, O. Berteau, *Front. Chem.* **2017**, *5*, DOI 10.3389/fchem.2017.00087.
[22] J. Bridwell-Rabb, B. Li, C. L. Drennan, *ACS Bio Med Chem Au* **2022**, acsbiomedchemau.1c00051.
[23] W. Ding, X. Ji, Y. Zhong, K. Xu, Q. Zhang, *Curr. Opin. Chem. Biol.* **2020**, *55*, 86–95.
[24] M. R. Bauerle, E. L. Schwalm, S. J. Booker, *J. Biol. Chem.* **2015**, *290*, 3995–4002.
[25] A. Benjdia, S. Pierre, C. Gherasim, A. Guillot, M. Carmona, P. Amara, R. Banerjee, O. Berteau, *Nat. Commun.* **2015**, *6*.
[26] P. A. Frey, *Trends in Res* **2018**, *1*, DOI 10.15761/TR.1000106.
[27] D. Deobald, L. Adrian, C. Schöne, M. Rother, G. Layer, *Sci. Rep.* **2018**, *8*, 7404.
[28] H. L. Knox, E. K. Sinner, C. A. Townsend, A. K. Boal, S. J. Booker, *Nature* **2022**, *602*, 343–348.
[29] W. J. Werner, K. D. Allen, K. Hu, G. L. Helms, B. S. Chen, S. C. Wang, *Biochemistry* **2011**, *50*, 8986–8988.
[30] B. J. Landgraf, E. L. McCarthy, S. J. Booker, *Annu. Rev. Biochem.* **2016**, *85*, 485–514.
[31] C. M. Jäger, A. K. Croft, *ChemBioEng Rev.* **2018**, *5*, 143–162.
[32] V. Kohler, N. J. Turner, *Chem. Commun.* **2015**, *51*, 450–464.
[33] L. W. Parks, F. Schlenk, *J. Biol. Chem.* **1958**, *230*, 295–305.
[34] N. Parveen, K. A. Cornell, *Mol. Microbiol.* **2011**, *79*, 7–20.
[35] T. Deguchi, J. Barchas, *J. Biol. Chem.* **1971**, *246*, 3175–3181.
[36] G. Markham, M. Pajares, *Cell Mol Life Sci* **2009**, *66*, 636–648.

[37] Z. J. Lu, G. D. Markham, *J. Biol. Chem.* **2002**, *277*, 16624–16631.
[38] A. S. Eustáquio, F. Pojer, J. P. Noel, B. S. Moore, *Nat. Chem. Biol.* **2008**, *4*, 69–74.
[39] J. Zhang, Y. G. Zheng, *ACS Chem. Biol.* **2016**, *11*, 583–597.
[40] F. Michailidou, A. Rentmeister, *Org. Biomol. Chem.* **2021**, *19*, 3756–3762.
[41] I. J. W. McKean, P. A. Hoskisson, G. A. Burley, *ChemBioChem* **2020**, *21*, 2890–2897.
[42] T. Davis, S. Kunakom, M. Burkart, A. Eustáquio, *Methods Enzymol.* **2018**, *604*, 367–388.
[43] M. A. Turner, X. Yang, D. Yin, K. Kuczera, R. T. Borchardt, P. L. Howell, *Cell Biochem. Biophys.* **2000**, *33*, 101–125.
[44] K. A. Cornell, W. E. Swarts, R. D. Barry, M. K. Riscoe, *Biochem. Biophys. Res. Commun.* **1996**, *228*, 724–732.
[45] T. D. Huber, B. R. Johnson, J. Zhang, J. S. Thorson, *Curr. Opin. Biotechnol.* **2016**, *42*, 189–197.
[46] H. Stecher, M. Tengg, B. J. Ueberbacher, P. Remler, H. Schwab, H. Griengl, M. Gruber-Khadjawi, *Angew. Chem. Int. Ed.* **2009**, *48*, 9546–9548.
[47] A. Ovcharenko, F. P. Weissenboeck, A. Rentmeister, *Angew. Chem. Int. Ed.* **2021**, *60*, 4098–4103.
[48] J. C. Sadler, L. D. Humphreys, R. Snajdrova, G. A. Burley, *ChemBioChem* **2017**, *18*, 992–995.
[49] N. Iwai, Y. Kitahara, T. Kitazume, *J. Mol. Catal. B Enzym.* **2011**, *73*, 1–4.
[50] B. J. C. Law, A.-W. Struck, M. R. Bennett, B. Wilkinson, J. Micklefield, *Chem. Sci.* **2015**, *6*, 2885–2892.
[51] J. Siegrist, S. Aschwanden, S. Mordhorst, L. Thöny-Meyer, M. Richter, J. N. Andexer, *ChemBioChem* **2015**, *16*, 2576–2579.
[52] J. Gagsteiger, S. Jahn, L. Heidinger, L. Gericke, J. N. Andexer, T. Friedrich, C. Loenarz, G. Layer, *Angew. Chem. Int. Ed.* **2022**, DOI 10.1002/anie.202204198.
[53] M. R. Challand, T. Ziegert, P. Douglas, R. J. Wood, M. Kriek, N. M. Shaw, P. L. Roach, *FEBS Lett.* **2009**, *583*, 1358–1362.
[54] M. R. Challand, F. T. Martins, P. L. Roach, *J Biol Chem* **2010**, *285*, 5240–5248.
[55] L. D. Palmer, D. M. Downs, *J. Biol. Chem.* **2013**, *288*, 30693–30699.
[56] S. Mordhorst, J. N. Andexer, *Nat. Prod. Rep.* **2020**, *37*, 1316–1333.
[57] S. Mordhorst, J. Siegrist, M. Müller, M. Richter, J. N. Andexer, *Angew. Chem. Int. Ed.* **2017**, *56*, 4037–4041.
[58] D. Popadić, D. Mhaindarkar, M. H. N. D. Thai, H. C. Hailes, S. Mordhorst, J. N. Andexer, *RSC Chem. Biol.* **2021**, *2*, 883–891.
[59] C. Liao, F. P. Seebeck, *Nat. Catal.* **2019**, *2*, 696–701.
[60] L. L. Bengel, B. Aberle, A.-N. Egler-Kemmerer, S. Kienzle, B. Hauer, S. C. Hammer, *Angew. Chem. Int. Ed.* **2021**, *60*, 5554–5560.
[61] K. H. Schülke, F. Ospina, K. Hörnschemeyer, S. Gergel, S. C. Hammer, *ChemBioChem* **2022**, *23*, e202100632.
[62] Q. Tang, C. W. Grathwol, A. S. Aslan-Üzel, S. Wu, A. Link, I. V. Pavlidis, C. P. S. Badenhorst, U. T. Bornscheuer, *Angew. Chem. Int. Ed.* **2021**, *60*, 1524–1527.
[63] J. Peng, C. Liao, C. Bauer, F. P. Seebeck, *Angew. Chem. Int. Ed.* **2021**, *60*, 27178–27183.
[64] A. Gross, O. Abril, J. M. Lewis, S. Geresh, G. M. Whitesides, *J. Am. Chem. Soc.* **1983**, *105*, 7428–7435.
[65] M. Hennig, L. G. Scott, E. Sperling, W. Bermel, J. R. Williamson, *J. Am. Chem. Soc.* **2007**, *129*, 14911–14921.
[66] U. Ngivprom, P. Lasin, P. Khunnonkwao, S. Worakaensai, K. Jantama, A. Kamkaew, R.-Y. Lai, *ChemBioChem* **2022**, cbic.202200071.

[67] S. Mordhorst, J. Singh, M. K. F. Mohr, R. Hinkelmann, M. Keppler, H. J. Jessen, J. N. Andexer, *ChemBioChem* **2019**, *20*, 1019–1022.
[68] J. N. Andexer, M. Richter, *ChemBioChem* **2015**, *16*, 380–386.
[69] H. K. Chenault, E. S. Simon, G. M. Whitesides, *Biotechnol. Genet. Eng. Rev.* **1988**, *6*, 221–270.
[70] Z. J. Lu, G. D. Markham, *J. Biol. Chem.* **2002**, *277*, 16624–16631.
[71] F. Wang, S. Singh, J. Zhang, T. D. Huber, K. E. Helmich, M. Sunkara, K. A. Hurley, R. D. Goff, C. A. Bingman, A. J. Morris, J. S. Thorson, G. N. Phillips, *FEBS J* **2014**, *281*, 4224–4239.
[72] W. H. Bowman, C. W. Tabor, H. Tabor, *Journal of Biological Chemistry* **1973**, *248*, 2480–2486.
[73] Y. Hanzawa, A. Imai, A. J. Michael, Y. Komeda, T. Takahashi, *FEBS Lett* **2002**, *527*, 176–180.
[74] M. Panicot, E. G. Minguet, A. Ferrando, R. Alcázar, M. A. Blázquez, J. Carbonell, T. Altabella, C. Koncz, A. F. Tiburcio, *Plant Cell* **2002**, *14*, 2539–2551.
[75] S. Bale, K. Baba, D. E. McCloskey, A. E. Pegg, S. E. Ealick, *Acta Crystallogr. D* **2010**, *66*, 181–189.
[76] J. W. Redmond, A. Tseng, *J. Chromatogr. A* **1979**, *170*, 479–481.
[77] R. L. Pajula, *Biochemical Journal* **1983**, *215*, 669–676.
[78] E. K. Sinner, D. R. Marous, C. A. Townsend, *ACS Bio Med Chem Au* **2022**, *2*, 4–10.
[79] N. J. Cosper, S. J. Booker, F. Ruzicka, P. A. Frey, R. A. Scott, *Biochemistry* **2000**, *39*, 15668–15673.
[80] S. Impano, H. Yang, E. M. Shepard, R. Swimley, A. Pagnier, W. E. Broderick, B. M. Hoffman, J. B. Broderick, *Angew. Chem. Int. Ed.* **2021**, *60*, 4666–4672.
[81] X. Ji, D. Mandalapu, J. Cheng, W. Ding, Q. Zhang, *Angew. Chem. Int. Ed.* **2018**, *57*, 6601–6604.
[82] X. Ji, Y. Li, L. Xie, H. Lu, W. Ding, Q. Zhang, *Angew. Chem. Int. Ed.* **2016**, *55*, 11845–11848.
[83] D. Mandalapu, X. Ji, Q. Zhang, *Biochemistry* **2019**, *58*, 36–39.
[84] R. Bonnett, *Chem. Rev.* **1963**, *63*, 573–605.
[85] F. Michailidou, N. Klöcker, N. Cornelissen, R. K. Singh, A. Peters, A. Ovcharenko, D. Kümmel, A. Rentmeister, *Angew. Chem. Int. Ed.* **n.d.**, *60*, 480–485.
[86] H. Yang, S. Impano, E. M. Shepard, C. D. James, W. E. Broderick, J. B. Broderick, B. M. Hoffman, *J. Am. Chem. Soc.* **2019**, *141*, 16117–16124.
[87] R. T. Borchardt, Y. S. Wu, *J. Med. Chem.* **1975**, *18*, 300–304.
[88] M. Dippe, W. Brandt, H. Rost, A. Porzel, J. Schmidt, L. A. Wessjohann, *Chem. Commun.* **2015**, *51*, 3637–3640.
[89] T. D. Huber, J. A. Clinger, Y. Liu, W. Xu, M. D. Miller, G. N. Phillips, J. S. Thorson, *ACS Chem. Biol.* **2020**, *15*, 695–705.
[90] A. J. Herbert, S. A. Shepherd, V. A. Cronin, M. R. Bennett, R. Sung, J. Micklefield, *Angew. Chem. Int. Ed.* **2020**, *59*, 14950–14956.
[91] E. Gasteiger, C. Hoogland, A. Gattiker, S. Duvaud, M. R. Wilkins, R. D. Appel, A. Bairoch, in *The Proteomics Protocols Handbook*, Humana Press, **2005**, pp. 571–607.
[92] U. K. Laemmli, *Nature* **1970**, *227*, 680–685.
[93] F. Muttach, A. Rentmeister, *Angew. Chem. Int. Ed.* **2016**, *55*, 1917–1920.
[94] I. R. Bothwell, M. Luo, *Org. Lett.* **2014**, *16*, 3056–3059.
[95] A. Breda, L. K. B. Martinelli, C. V. Bizarro, L. A. Rosado, C. B. Borges, D. S. Santos, L. A. Basso, *PLoS ONE* **2012**, *7*, e39245.

770 [96] F. Michailidou, N. Klöcker, N. V. Cornelissen, R. K. Singh, A. Peters, A. Ovcharenko, D. Kümmel, A. Rentmeister, *Angew. Chem. Int. Ed.* **2021**, *60*, 480–485.
[97] H. Liu, Y. Jiang, Y. Luo, W. Jiang, **2006**, 4.
[98] M. T. Marty, A. J. Baldwin, E. G. Marklund, G. K. A. Hochberg, J. L. P. Benesch, C. V. Robinson, *Anal. Chem.* **2015**, *87*, 4370–4376.
775

Acknowledgements:
We thank Katharina Strack (University of Freiburg) for her skilful technical assistance. Jaspreet Chahal (University of Southampton) and Sonya Danesh (University of Freiburg) are acknowledged for help with optimisation of *rppk* production, and Dr Manfred Keller and Dr
780 Thomas Haas (University of Freiburg) for help with NMR measurements. We also thank Dr Peter Roach for helpful advice on radical SAM chemistry. Dr Florian Hubrich (ETH Zurich) is thanked for proofreading and helpful discussions.
This work was funded by the European Research Council (ERC project 716966; L.G., D.M., L.K., J.N.A.), Deutsche Forschungsgemeinschaft (RTG1976; L.K., J.G., G.L., J.N.A.;
785 IRTG2027 N.C., A.R.). X.W. is the recipient of a PhD stipend from the Camille Henry Dreyfus Foundation.

Author contributions

JNA conceived and designed the study, supported by LG, DM, LK and SM. LG, DM, and LK
790 planned and performed experiments regarding ribose phosphorylation, cofactor supply and regeneration with MTs and radical SAM enzymes, supported by JG and GL. MK and MKFM planned and performed experiments regarding APTs, supported by XW and FPS. NVC and AR supported experiments with SAM analogues. LG, DM, LK, SJ, MK, and MKFM analysed the data. LG, DM, and LK interpreted the data, supported by MK, MKFM, SJ, CL, HJJ, and
795 JNA. JNA, LG, and DM wrote the manuscript, supported by SM, HJJ, AR, GL, FPS, and CL. All authors reviewed and approved the final manuscript.

Conflict of interest

The authors declare no competing interests.

800